# Charge carriers in the divalent conductor (BEDT-TTF)$Cu_2Br_4$

H. Ito, Y. Yokochi, H. Tanaka, and S. Kuroda
*Department of Applied Physics, Nagoya University, Chikusa, Nagoya, 464-8603, Japan*

R. Kanehama, M. Umemiya, H. Miyasaka, K-I. Sugiura, and M. Yamashita*
*Department of Chemistry, Tokyo Metropolitan University and CREST, 1-1 Minami-Ohsawa, Hachioji 192-0397, Japan*

H. Tajima and J. Yamaura
*Institute of Solid State Physics, University of Tokyo, Kashiwa, Chiba 277-8581, Japan*
(Received 24 September 2004; revised manuscript received 19 November 2004; published 15 February 2005)

An organic semiconductor (BEDT-TTF)$Cu_2Br_4$ exhibits rather high conductivity ($10^{-2}$ S/cm with little sample dependence) despite the fact that BEDT-TTF molecules have a divalent closed-shell state as evidenced by ESR and Raman measurements. In order to obtain insight into the properties of the charge carriers, the Hall coefficient for the semiconductor was measured in the temperature range of 120–300 K. Charge carriers are electronlike and their concentration is rather low [$(4\pm2)\times10^{19}$ /mol at room temperature]. The carrier concentration increases exponentially with temperature with an activation energy of 0.17 eV below 170 K and 0.12 eV above 170 K. The Hall mobility is as high as 2 $cm^2$/Vs, supporting the high conductivity of the material. Thermo-electric power measurements also support the sign and concentration of the charge carriers. The carrier concentration at room temperature is one order of magnitude lower than the concentration of Curie spin due to the presence of $\pi$ electrons at low temperatures. The fine structure of the ESR signal from the Curie spin shows smearing above 100 K. This behavior is caused by exchange interaction mediated via conduction electrons. These results indicate that charge carriers localized at low temperatures are thermally activated to the conduction band at high temperatures. The possible origins of the charge carriers are discussed in terms of impurity sites of the different crystal phases of (BEDT-TTF)$_2$[$Cu_4Br_6$(BEDT-TTF)] in the matrix.

DOI: 10.1103/PhysRevB.71.085202 PACS number(s): 72.80.Le, 76.30.−v, 72.20.Jv

## I. INTRODUCTION

The $\pi$-conjugated molecule of bis(ethylenedithio)tetrathiafulvalene (BEDT-TTF) has been widely studied as a constituent of a large number of conducting and superconducting cation-radical salts.[1] In these salts, BEDT-TTF molecules become donors coupled with appropriate acceptor molecules, and charge transfer occurs between them. It is widely believed that in order to realize electrical conduction in charge transfer salts, incomplete charge transfer between donors and acceptors is important so as to have an intermediately-filled conduction band comprised of overlapping highest-occupied molecular orbitals (HOMO) of the BEDT-TTF molecules. Charge transfer salts made of BEDT-TTF molecules yielding high conductivity values are often formed where the oxidation state of BEDT-TTF ranges from +1/2 to +1. All superconducting examples discovered so far have donor oxidation states of +1/2 or +2/3.

Recently, Kanehama synthesized a series of charge transfer salts by a direct redox reaction of BEDT-TTF and $Cu^{II}Br_2$.[2] These salts are semiconductors with rather high conductivities on the order of 1 to $10^{-4}$ S/cm at room temperature (two of them show metallic conduction near room temperature). Among the reported salts, (BEDT-TTF)$Cu_2Br_4$, (BEDT-TTF)$_2Cu_6Br_{10}$, (BEDT-TTF)$_2Cu_3Br_7(H_2O)$, and (BEDT-TTF)$_2Cu_6Br_{10}(H_2O)_2$ are very interesting in the sense that the valence state of BEDT-TTF is 2+ for the above four salts, provided that Cu ions are reduced to a monovalent state in order to oxidize BEDT-TTF. In these salts, charge transfer between BEDT-TTF and anion molecules is completed resulting in an exhausted HOMO band. The rather good electrical conductivity of these salts clearly contradicts the situation that BEDT-TTF has a closed-shell state with no electrons in the HOMO band. There are only few preceding examples of BEDT-TTF salts with divalent BEDT-TTF, (BEDT-TTF)$(BF_4)_2$ and (BEDT-TTF)$(ClO_4)_2$, and more recently (BEDT-TTF)[$Fe(CN)_4(CO)_2$], but they are all insulators with conductivities less than $10^{-5}$ S/cm.[3–5]

In the divalent salts reported by Kanehama *et al.*, BEDT-TTF molecules are coordinated directly to the Cu ion of the anion cluster in a monodentate or bidentate manner, similar to (BEDT-TTF)$Cu_2Br_3$.[6] The direct bonding between BEDT-TTF molecules and anions forming a "fused-$\pi$-*d* system" is another remarkable feature of these salts. The $\pi$-*d* interactions between the $\pi$-electrons of BEDT-TTF and the *d*-electrons of the Cu ion will be enhanced by the direct bonding, similar to observations in the Cu(DCNQI)$_2$ system in which the metal-insulator transition is caused by the occurrence of a mixed valence state of Cu.[7]

Among the four divalent salts mentioned above, large single crystals suitable for electronic property measurements are available only for the first salt, that is (BEDT-TTF)$Cu_2Br_4$. In Fig. 1, we show the crystal structure of (BEDT-TTF)$Cu_2Br_4$.[2] The space group is $P2_{1/n}$. The unit-cell parameters are $a=9.401(7)$ Å, $b=10.841(8)$ Å, $c=10.035(8)$ Å, $\beta=98.48(1)°$, $V=1011.7(1)$ Å$^3$ and $Z=2$. The space group is the same as for the former examples

 

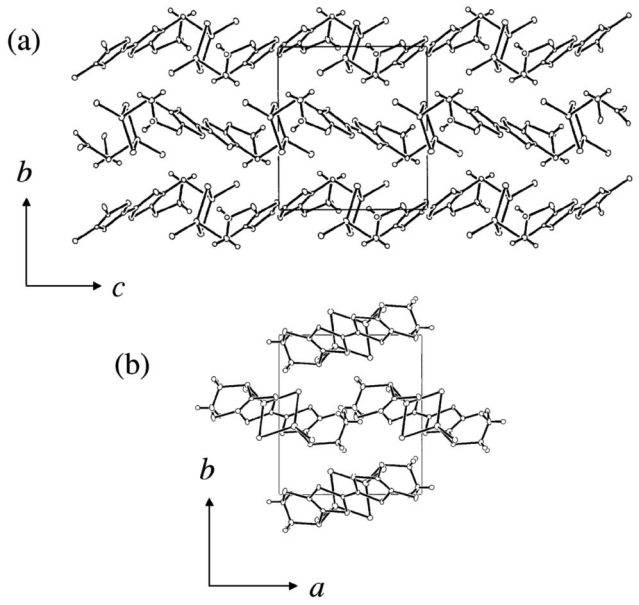


FIG. 1. Crystal structure of (BEDT-TTF)$Cu_2Br_4$ projected on *b*-*c* (a) and *a*-*b* (b) planes.

of divalent salts of (BEDT-TTF)$(BF_4)_2$ and (BEDT-TTF)$(ClO_4)_2$, but the unit cell size is larger for (BEDT-TTF)$Cu_2Br_4$ because of the larger size of the anion cluster of $Cu_2Br_4^{2-}$. In (BEDT-TTF)$Cu_2Br_4$, the S atoms of the BEDT-TTF molecules are coordinated directly to the Cu atoms of the $Cu_2Br_4^{2-}$ anion clusters with a bond length of 2.38 Å, forming a chain structure along the *c* axis. BEDT-TTF molecules are *cis*-bidentate ligands to $Cu_2Br_4^{2-}$ anion clusters.

In this paper, we present detailed studies of the electrical conductivity, ESR measurements, Raman measurements, the Hall coefficient, and thermoelectric power measurements for (BEDT-TTF)$Cu_2Br_4$ in order to obtain insights into the origins of charge carriers and the mechanism of electrical conduction. The valence state of BEDT-TTF is confirmed to be 2+ by ESR and Raman measurements. The concentration of charge carriers is found to be as low as one carrier per $10^4$ molecules, but the mobility is high enough to support the high conductivity. The fine structure of the ESR line shape at low temperatures is smeared out above 100 K. The results are discussed in terms of the charge carriers thermally activated from impurity sites of the different crystal phases in the material.

## II. EXPERIMENT

Black needle (BEDT-TTF)$Cu_2Br_4$ single crystals were grown by direct oxidization of BEDT-TTF by $Cu^{II}Br_2$ under the condition that slow diffusive reaction between solutions of BEDT-TTF in THF ($2.6\times10^{-2}$ M) and $Cu^{II}Br_2$ in methanol ($9.0\times10^{-2}$ M) occurs.[2,8] After several weeks, single crystals with a typical size of $2\text{mm}\times0.05\text{mm}\times0.05\text{mm}$ were harvested. The needle axis corresponds to the *c* axis. The cross section of the needle is usually a square with edges of [110] and [1$\bar{1}$0] crystallographic axes. Platelike crystals of another phase of (BEDT-TTF)$_2$[$Cu_4Br_6$(BEDT-TTF)] are obtained as a low-yield coproduct for low concentrations ($1.1\times10^{-2}$ M) of $Cu^{II}Br_2$ solution.[2,8]

The temperature dependence of electrical conductivity was measured using the four-probe dc method with a measuring current of 0.1–0.01 mA applied along the *c* axis, with a typical cooling rate of 1 K/min. The temperature was monitored with calibrated carbon-glass or Cernox thermistors. The measuring current was alternated in order to eliminate thermoelectric effects. The electrical conductivity under pressure was measured with a Be-Cu clamp-type cell. Pressure was applied via Daphne 7373 oil at room temperature and clamped with screws. The pressure value decreases by ~0.2 GPa at low temperatures compared to that at room temperature.

ESR measurements were performed using a Bruker EMX X-band spectrometer equipped with an OXFORD ESR900 gas flow cryostat for temperatures between room temperature and 5 K. Since the ESR signal from each (BEDT-TTF)$Cu_2Br_4$ crystal is small, 40 single crystals were aligned along the *c* axis on a mylar (polyethylene-terephthalate) substrate under a microscope, with a small amount of silicon grease to fix them. The crystal surface was not aligned, and was either [110] or [1$\bar{1}$0]. The dc magnetic field of the ESR spectrometer was thus applied along the [110] direction for some samples and [1$\bar{1}$0] for others. The absolute magnitude of the susceptibility and *g*-value were calibrated using $CuSO_4\cdot5H_2O$ and diphenylpicrylhydrazyl (DPPH) as standards, respectively.

Raman spectra were measured in air using a Renishaw Ramascope system 1000 with an He-Ne (632.8 nm) laser incident on the [110] surface with polarization perpendicular to the *c* axis.

The Hall coefficient was measured using the four terminal dc technique with a PPMS system (Quantum Design) equipped with a bipolar 9 T magnet. The magnetic field was applied perpendicular to the crystal surface, that is, along the [110] or [1$\bar{1}$0] direction. A current of 0.1 mA was applied along the *c* axis and the voltage across the needle was measured. The measuring current was alternated in order to eliminate thermoelectric effects. The Hall coefficients were calculated by a linear fit of the difference in Hall voltages under two opposite directions of the external magnetic field swept from $-9$ to 9 T. During the magnetic field sweep, temperature was controlled with an accuracy of $\pm5$ mK.

The thermoelectric power was measured with an MMR Seebeck measurement system equipped with an $N_2$ high pressure gas cooling system. A Cu-constantan differential thermocouple was used to monitor the temperature gradient. The typical temperature gradient was 1 to 2 K along the *c* axis.

## III. RESULTS

### A. Conductivity measurements

In Fig. 2, we show the temperature dependence of electrical conductivity under different hydrostatic pressures up to a maximum of 1 GPa. The conductivity shows thermally acti-

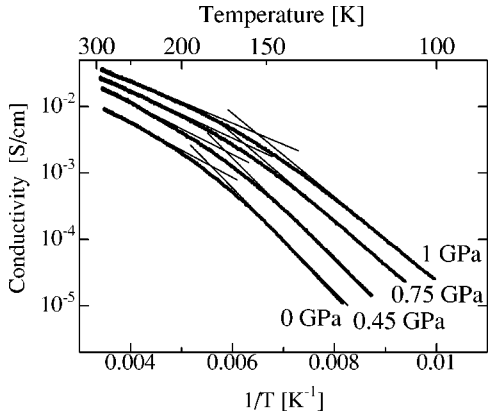


FIG. 2. Temperature dependence of conductivity of (BEDT-TTF)$Cu_2Br_4$ under various values of the hydrostatic pressure up to 1 GPa. The pressure values are those at room temperature. At lower temperatures, the pressure is reduced by ~0.2 GPa. Thin asymptotic lines on each curve represent thermally-activated temperature dependence.

vated behavior, however, the data cannot be explained by a single activation energy. The activation energy changes at about 170 K; it is 0.16 eV below 170 K and 0.09 eV above 170 K at ambient pressure. This behavior is observed for all the sample crystals studied. The observed temperature dependence of electrical conductivity cannot be explaned with a different model such as the variable range hopping model. Under pressure, the conductivity increases by up to one order of magnitude. The crossover temperature of the activation energy change shifts to a lower temperature of 150 K at 1 GPa. The activation energy is reduced about 30% for each temperature range for an applied pressure of 1 GPa. The overall temperature dependence of conductivity is unchanged under pressures of up to 1 GPa.

The anisotropy of the conduction is evaluated using the Montgomery method.[9] The conductivity along the *c* axis is about ten times as large as the conductivity perpendicular to the *c* axis, which is in agreement with former two-probe measurements.[2] The anisotropy of conductivity is almost unchanged at low temperatures down to 150 K, below which measurement was impossible because of the limitation in terms of the input impedance of the voltmeter used. In spite of the one-dimensional chain structure, the anisotropy of the conduction is not as high as in other one-dimensional materials such as TTF-TCNQ and platinum complexes. According to tight-binding band calculations,[10] interchain transfer integrals mediated by overlaps of BEDT-TTF orbitals on adjacent chains are larger than the intrachain transfer integrals between BEDT-TTF orbitals. The band dispersion is one dimensional along the *a*-axis direction, if we take into account only the BEDT-TTF orbitals. However, if we fully take the intrachain transfer integrals between BEDT-TTF and $Cu_2Br_4$ orbitals into account, the band dispersion is three dimensional.[11] Experimental results show that the direction of most conduction is the *c* axis and the conductivity anisotropy is rather low indicating that there must be a contribution of the anion orbital to the electrical conduction along the *c* axis.

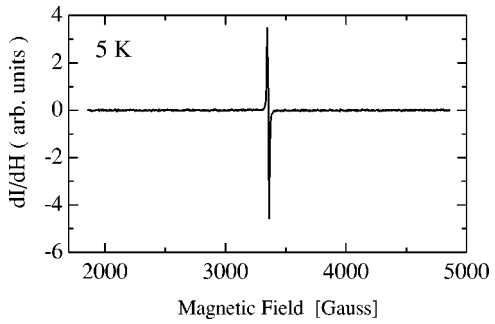


FIG. 3. ESR spectrum at 5 K of 40 aligned single crystals of (BEDT-TTF)$Cu_2Br_4$ in a wide field range.

### B. Valence state of Cu and BEDT-TTF

Figure 3 shows an ESR spectrum at 5 K for the 40 aligned single crystals as described earlier. The external field is applied along the [110] or [1$\bar{1}$0] axis for each crystal. The sharp signal near $g=2.01$ is ascribed to the $\pi$-electron on the BEDT-TTF molecule. No other signal was observed at other *g* values in this experiment. This indicates that the Cu ions are nonmagnetic and monovalent. The average valence of the BEDT-TTF molecules is thus considered to be 2+. The 2+ valence state of BEDT-TTF is consistent with the central C=C bond length of 1.43 Å, found by x-ray analysis.[2,4]

In Fig. 4, we show a Raman spectrum under He-Ne Laser excitation, polarized perpendicular to the *c* axis at room temperature. Among the observed Raman signals, $\nu_2$, $\nu_3$, $\nu_5$, $\nu_6$, $\nu_7$, and $\nu_9$ can be assigned to major $a_g$ mode molecular vibrations of BEDT-TTF. The $a_g$ mode molecular vibrations are known to be sensitive to the charge concentration on HOMO of BEDT-TTF.[12] In the present salt, these are observed at 1383, 1310, 1298, 943, 916, and 530 $cm^{-1}$, respectively. These Raman shifts are in good agreement with the results for the divalent salt of (BEDT-TTF)$(ClO_4)_2$,[13] indicating that the present salt is composed mainly of divalent BEDT-TTF molecules.

In Fig. 5, we show the temperature dependence of the spin susceptibility from $\pi$-electrons calculated by integrating the first-derivative ESR signal twice near $g=2.01$. The susceptibility obeys the Curie law at low temperatures with a Curie constant of $C=2.4\times10^{-5}$ emu K/mol. By using the formula

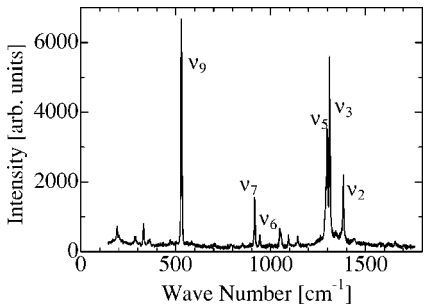


FIG. 4. Raman spectrum at room temperature of a single crystal of (BEDT-TTF)$Cu_2Br_4$ under He-Ne laser excitation, polarized perpendicular to the *c* axis.

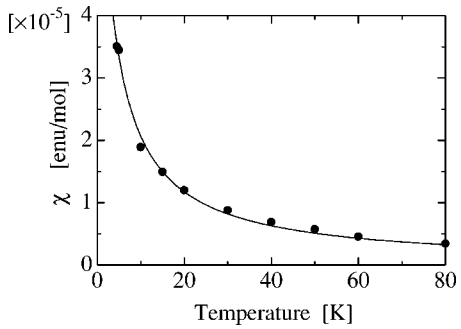


FIG. 5. Temperature dependence of the $\pi$-electron spin susceptibility. The solid line is a fit to the Curie law.

$$C = \frac{\mu_B^2 g^2 n S(S+1)}{3k_B}, \tag{1}$$

where $\mu_B$ is the Bohr magneton and $k_B$ is the Boltzmann constant, the concentration of localized spins at low temperature is evaluated. With $S=1/2$, the spin concentration is evaluated to be $n=4.3\times10^{20}$/mol. This is a very low concentration of 1 spin per $1.4\times10^3$ BEDT-TTF molecules. The low concentration of spins is consistent with the fact that the majority of the BEDT-TTF molecules are divalent. Spins of $\pi$-electrons are localized at trapped sites in the low temperature region.

### C. Hall coefficient

In order to measure the carrier concentration, we carried out Hall coefficient measurements. The carrier polarity was negative. The carrier concentration was $(4\pm2)\times10^{19}$/mol at room temperature. This is very low carrier concentration of the order of one carrier per $10^4$ molecules, one order of magnitude lower than that of the Curie spins. In Fig. 6, we show the temperature dependence of Hall carrier concentrations for three different single crystals. The carrier concentration increased exponentially with temperature with an activation energy of $0.17\pm0.01$ eV below 170 K and $0.12\pm0.01$ eV above 170 K. Similar to the conductivity measurements, the activation energy changes its value at about 170 K. This

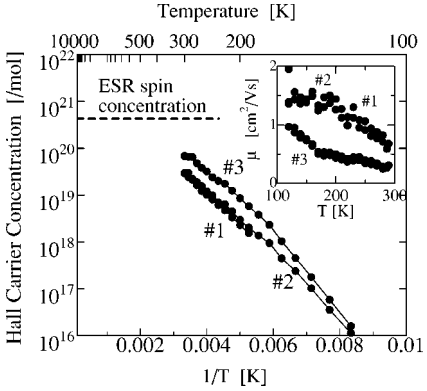


FIG. 6. Temperature dependence of the Hall carrier concentrations for three different single crystals. Inset: Hall carrier mobility of the three samples calculated by the relation $\sigma=ne\mu$.

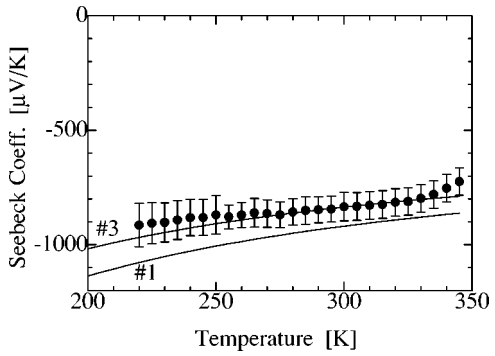


FIG. 7. Temperature dependence of Seebeck coefficients of (BEDT-TTF)$Cu_2Br_4$. The two solid lines in the figure are calculated by Eq. (2) using the Hall carrier concentrations of sample no. 1 and no. 3 in Fig. 6.

indicates that the dominant term determining the temperature dependence of $\sigma$ is $n$ but not $\mu$.

As shown in Fig. 6, the carrier concentration tends to approach the spin concentration found by low temperature ESR measurements at the high temperature limit. This result implies a scenario wherein the spins localized at low temperature are activated thermally to be charge carriers at high temperatures. Some part of the observed spins contribute to the electrical conduction and others do not, depending on the temperature. A detailed discussion will be presented in the next section in terms of the temperature dependence of the ESR line shape.

Using the conductivity $\sigma$ at ambient pressure shown in Fig. 1 and the carrier concentrations of the three samples given above, we calculated the Hall mobility $\mu$ using the relation $\sigma=ne\mu$, as shown in the inset of Fig. 6. The mobility was $0.5\pm0.2$ cm$^2$/Vs at room temperature and increased weakly with decreasing temperature up to a value as high as 2 cm$^2$/Vs at 120 K.

### D. Seebeck coefficient

In Fig. 7, we show the temperature dependence of the Seebeck coefficient. A negative sign indicates that the carriers are electronlike. The solid lines in the figure are calculations according to the formula for fermions under on-site Coulombic repulsion,[14]

$$S = -\frac{k_B}{e}\ln\left[\frac{2(1-\rho)}{\rho}\right] \tag{2}$$

using the carrier concentrations $\rho$ of the sample no. 1 and no. 3 shown in Fig. 6. The sign and the absolute value of the Seebeck coefficient are in good agreement with the Hall measurements.

## IV. DISCUSSION

### A. Temperature dependence of the carrier concentration

The carrier concentration found by the Hall measurements increased exponentially with temperature. The activation energy of the carrier concentration changed at around 170 K, at

which the activation energy found by the conductivity measurement also changed, as shown in Fig. 2. The gradual change in activation energy at 150–170 K was observed even under pressure. Because of the gradual and crossover like behavior and insensitivity to pressure, an electronic phase transition as suggested in (TTMTTF)$Cu_2Br_{4.72}$ (Ref. 15) cannot be considered to be the origin of the change in activation energy. It is probable that there are two kinds of different carrier traps, deep and shallow. At low temperatures, carriers are trapped at deep trap sites. At elevated temperatures, the effective depth of the trapped sites become shallow with help of phonons.

In the meantime, the change in apparent activation energy of the charge carriers may also be explained in terms of the extrinsic semiconductor in which both donor and acceptor impurities are present with concentrations of $N_D$ and $N_A$, respectively ($N_D \gg N_A$), as is commonly found in standard semiconductor textbooks.[16] At low temperatures, the carrier concentration $n$ is lower than $N_A$, and the carrier concentration can be formulated as

$$n = n_0 \exp\left[ - \frac{E_c - E_D}{k_B T} \right], \tag{3}$$

where $E_c$ and $E_D$ are the energy of the conduction band edge and donor ionization, respectively. On the other hand, at the intermediate temperature region in which the carrier concentration increases more than the acceptor concentration, $N_D \gg n \gg N_A$, the carrier concentration can be formulated as

$$n = n_0 \exp\left[ - \frac{E_c - E_D}{2k_B T} \right]. \tag{4}$$

The apparent activation energy defined by the Arrhenius plot of the carrier concentration differs twice between that in the low temperature $N_D \gg N_A \gg n$ regime and that in the intermediate temperature $N_D \gg n \gg N_A$ regime. The difference in apparent activation energy below and above 170 K may be ascribed to the two different regimes of the extrinsic semiconductor. In the high temperature regime, wherein all the carriers are activated, carrier concentration is independent of temperature in the so-called exhausted regime. Since the Hall carrier concentration still increases at room temperature, the room temperature is still in the intermediate temperature regime. It is possible that the exhausted regime exists above room temperature, where all the spins found by low temperature ESR measurements will be thermally-activated eventually to be charge carriers. As donor sites, impurity sites of a different phase of the crystal (BEDT-TTF)$_2$[$Cu_4Br_6$(BEDT-TTF)] are considered, as discussed in the next subsection. As acceptors, a very small concentration of the anion defect is the candidate. Structural studies directly specifying the carrier trap sites in the crystal, using STM for example, would be helpful in the future in order to study the origin of the temperature dependence of the carrier concentration.

Aside from the nature of the carrier trap sites, it is notable that the mobility of the charge carriers is rather high. Since the mobility increases at low temperatures, the carrier conduction is bandlike. Charge carriers, once they get out of the trapping sites, become highly mobile. They are activated to the conduction band made of overlapping HOMO orbitals of BEDT-TTF.

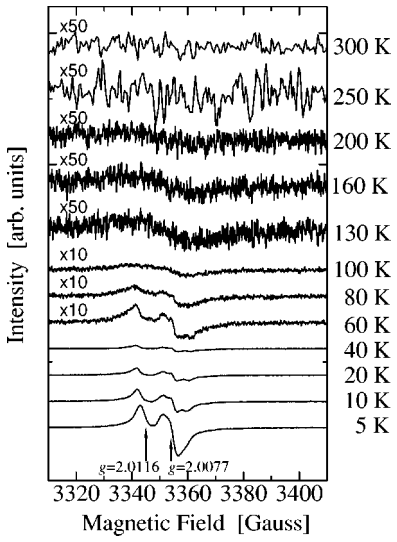


FIG. 8. ESR spectra from 5 K to 300 K of 40 aligned single crystals of (BEDT-TTF)$Cu_2Br_4$ near $g=2.01$. ESR spectrum above 60 K, and above 130 K, are multiplied by factors of 10 and 50, respectively. Base lines of each signal are shifted for clarity.

### B. Exchange smearing of the Curie spin ESR signal

In order to confirm that Curie spins are activated to be charge carriers at higher temperatures, we can examine the temperature dependence of the ESR line shape. This temperature dependence provides a crucial probe for revealing microscopic information, since it reflects the dynamical information of spins such as spin motion or exchange interaction mediated by mobile electrons. Figure 8 shows line shapes of the ESR signals from $\pi$ electrons at different temperatures from 5 K to 300 K. A line shape consists of two distinct major lines of $g=2.0116$ and $g=2.0077$ with some fine structure at low temperatures. The structure of the line shape becomes obscure above 100 K and merges into a single line as seen in the figure. The ESR signal eventually diminishes above 200 K.

First, we discuss the origin of the fine structure of ESR signals at low temperature where spins are expected to be localized at trapped sites. There are two different orientations of the BEDT-TTF molecules in the crystal, as shown in Fig. 1(b). Therefore there are two different molecular orientations with respect to the applied magnetic field direction. The $g$ values for the two orientations calculated with direction cosines with respect to the magnetic field direction along [110] are 2.0066–2.0076 and 2.0066–2.0069, respectively, based on the principal values of the BEDT-TTF cation radical.[17,18] Owing to the symmetry of the crystal, $g$ values are expected to be the same for the magnetic field along $[1\bar{1}0]$. Therefore, the difference in the $g$ values between the two orientations is at most $\Delta g = 0.001$. The difference in the $g$ values of the ESR signals observed in Fig. 8, $\Delta g \sim 0.004$, is too large to be ascribed to the two different orientations of BEDT-TTF mol-

ecule in the (BEDT-TTF)$Cu_2Br_4$ crystal. The trapping site for the spin is not the matrix of the crystal itself but an imperfection or an impurity, at least for the signal at $g=2.0116$. For the origin of trapped spins, one typical explanation is a partial charge transfer from Cu to BEDT-TTF. However, we observed no ESR signals corresponding to $Cu^{2+}$ as shown in Fig. 3, indicating that the concentration of the $Cu^{2+}$ is too small and out of the detection range of the present ESR spectrometer. The partial charge transfer from Cu to BEDT-TTF cannot account for the observed concentration of unpaired electrons. Another possible explanation is that a different phase of the crystal (BEDT-TTF)$_2$[$Cu_4Br_6$(BEDT-TTF)] may be co-grown partially among the (BEDT-TTF)$Cu_2Br_4$ matrix. This is probable since the crystal of (BEDT-TTF)$_2$[$Cu_4Br_6$(BEDT-TTF)] is obtained depending on subtle differences in the growth condition from that of (BEDT-TTF)$Cu_2Br_4$.[8]. In (BEDT-TTF)$_2$[$Cu_4Br_6$(BEDT-TTF)], the average valence of BEDT-TTF molecules is $+2/3$ giving ESR signals.[8] Since $g$ values different from those of (BEDT-TTF)$Cu_2Br_4$ are observed, it is natural to regard that spin-trapping sites are inclusions of the (BEDT-TTF)$_2$[$Cu_4Br_6$(BEDT-TTF)] domain at which electronically active BEDT-TTF molecules are aligned like (BEDT-TTF)$_2$[$Cu_4Br_6$(BEDT-TTF)]. Further fine structure visible above 10 K may be caused by misorientation of such a (BEDT-TTF)$_2$[$Cu_4Br_6$(BEDT-TTF)] domain with respect to the matrix crystal. The presence of nonstoichiometric impurity sites with concentrations as low as 0.1% is not unlikely in BEDT-TTF salts. In $\kappa$-(BEDT-TTF)$_2$Cu(NCS)$_2$, such impurity sites are considered to be the origin of the temperature width of the superconductivity transition.[19]

Above 100 K, the structure of the ESR signal from the $\pi$ electron is smeared away and merges into a single signal. This smearing of the structure indicates exchange interaction among spins that yield each ESR signal. Direct spin-spin interaction in this crystal is almost impossible because the Curie concentration of 1 spin per $1.4\times10^3$ molecules is too low. Therefore mediation by mobile spin is essential to couple isolated spins with different $g$ values. If we assume that the exchange interaction between a localized electron (spin) and a conduction electron is sufficiently strong, the smearing of the ESR fine structure is understood as being caused by the exchange interaction. The exchange-coupling condition between two localized spins mediated via conduction electrons is $\Delta\omega\tau\ll1$, where $\Delta\omega$ is the frequency separation of two localized spins with different $g$ values and $\tau$ is the hopping time of the conduction electron at each site.[20] Considering the frequency of the X-band spectrometer (9.4 GHz), frequency separation for $\Delta g=0.004$ is 35 MHz. The hopping time $\tau$ is related to the diffusive mobility valid at the bottom of the conduction band,

$$\mu=\frac{a^2e}{\tau k_BT}, \tag{5}$$

where $a$ is the lattice constant. According to Eq. (5), a conduction electron moving faster than a mobility of $10^{-5}$ $cm^2/Vs$ satisfies the exchange-coupling condition. In the salt used in this study, the mobility of charge carriers is of the order of 1 $cm^2/Vs$ and is far greater than this criterion. Electronic carriers with spins are excited from the carrier traps and move freely above 100 K mediating the exchange interaction among the impurity sites, (BEDT-TTF)$_2$[$Cu_4Br_6$(BEDT-TTF)] domains in the crystal, which yields ESR signals with fine structures at low temperatures. The thermally activated mobile spin is the origin of the charge carrier resulting in the high conductivity of the present salt.

## V. CONCLUSIONS

The electrical conduction of and origin of charge carriers for a divalent BEDT-TTF salt of (BEDT-TTF)$Cu_2Br_4$ is studied. Electrical conductivity, ESR, Hall carrier and thermoelectric power measurements all show the presence of electronic carriers in spite of the closed-shell structure of divalent BEDT-TTF molecules. Electronic carriers trapped at low temperature are thermally activated to the conduction band made of overlapping HOMO of BEDT-TTF molecules and contribute to the electrical conduction. In terms of the origin of the carrier traps at low temperatures, possible impurity sites of a different phase of the crystal (BEDT-TTF)$_2$[$Cu_4Br_6$(BEDT-TTF)] are considered.

## ACKNOWLEDGMENTS

The authors thank U. Mizutani, H. Ikuta, and T. Takami for the use of their facilities and experimental support for Hall and thermoelectric power measurements. The authors also thank T. Mori for discussions on the band structure. The Raman measurements were performed using facilities of the Institute for Solid State Physics, the University of Tokyo. This research was supported by the Ministry of Education, Culture, Sport, Science and Technology, Grant-in-Aid for Young Scientists (B) 15740210, and Scientific Research on Priority Areas "Novel Functions of Molecular Conductors Under Extreme Conditions," 16038215.

*Present address: Department of Chemistry, Tohoku University, Aoba, Sendai 980-8578, Japan.

[1] T. Ishiguro, K. Yamaji, and G. Saito, *Organic Superconductors*, 2nd ed. (Springer-Verlag, Berlin, 1998).

[2] R. Kanehama, M. Umemiya, F. Iwahori, H. Miyasaka, K.-i. Sugiura, M. Yamashita, Y. Yokochi, H. Ito, S. Kuroda, H. Kishida, H. Okamoto, and M. Kaneko, Inorg. Chem. **42**, 7173 (2003).

[3] K. A. Abboud, M. B. Clevenger, G. F. de Oliveira, and D. R. Talham, J. Chem. Soc., Chem. Commun. **1993**, 1560.

[4] L. K. Chou, M. A. Quijada, M. B. Clevenger, G. F. de Oliveira,

K. A. Abboud, D. B. Tanner, and D. R. Talham, Chem. Mater. **7**, 530 (1995).
[5] X. Xiao, H. Xu, W. Xu, D. Zhang, and D. Zhu, Synth. Met. **144**, 51 (2004).
[6] M. B. Inoue, M. Inoue, M. A. Bruck, and Q. Fernando, J. Chem. Soc., Chem. Commun. **1992**, 515.
[7] H. Kobayashi, A. Miyamoto, R. Kato, F. Sakai, A. Kobayashi, Y. Yamakita, Y. Furukawa, M. Tasumi, and T. Watanabe, Phys. Rev. B **47**, 3500 (1993).
[8] R. Kanehama, Master thesis, Tokyo Metropolitan University, 2003 (in Japanese).
[9] H. C. Montgomery, J. Appl. Phys. **42**, 2971 (1971).
[10] T. Mori, A. Kobayashi, Y. Sasaki, H. Kobayashi, G. Saito, and H. Inokuchi, Bull. Chem. Soc. Jpn. **57**, 627 (1984).
[11] T. Mori (private communication).
[12] H. H. Wang, J. R. Ferraro, J. M. Williams, U. Geiser, and J. A. Schlueter, J. Chem. Soc., Chem. Commun. **1993**, 1560.
[13] H. H. Wang, A. M. Kini, and J. M. Williams, Mol. Cryst. Liq. Cryst. Sci. Technol., Sect. A **284**, 211 (1996).
[14] P. M. Chaikin and G. Beni, Phys. Rev. B **13**, 647 (1976).
[15] I. Olejniczak, W. Pukacki, A. Graja, Y. Q. Liu, S. G. Liu, and D. B. Zhu, Synth. Met. **94**, 51 (1998).
[16] For example, K. Seeger, *Semiconductor Physics - An Introduction*, 9th ed. (Springer, Berlin, 2004).
[17] N. Kinoshita, M. Tokumoto, H. Anzai, and G. Saito, J. Phys. Soc. Jpn. **54**, 4498 (1985).
[18] T. Sugano, G. Saito, and M. Kinoshita, Phys. Rev. B **34**, 117 (1986).
[19] J. Singleton, N. Harrison, C. H. Mielke, J. A. Schlueter, and A. M. Kini, J. Phys.: Condens. Matter **13**, L899 (2001).
[20] C. Kittel, *Introduction to Solid State Physics*, 7th ed. (Wiley, New York, 1996), Chap. 16.